ELSEVIER

Tribology International 34 (2001) 815–822

TRIBOLOGY INTERNATIONAL

www.elsevier.com/locate/triboint

Study of thin surfactant films under shear using the tribological surface force apparatus

K. Boschkova [a, b,*], B. Kronberg [b], M. Rutland [a], T. Imae [c]

[a] *Department of Chemistry, Surface Chemistry, Royal Institute of Technology, Drottning Kristinas väg 51, SE-100 44 Stockholm, Sweden*
[b] *YKI, Institute for Surface Chemistry, Box 5607, SE-114 86 Stockholm, Sweden*
[c] *Research centre for Materials Science, Nagoya University, Chikusa, Nagoya 464-8602, Japan*

Abstract

Static and dynamic behaviour of thin surfactant films in aqueous solution of hexadecyltrimethylammonium salicylate (C16TASal) were investigated using the tribological surface force apparatus. Normal force measurements show that 0.15 mM C16TASal builds up an innermost film of approximately 8–11 Å thickness at each mica surface, indicating that the surfactant adsorbs in a flat conformation. Furthermore, the height of the force barrier at approximately 60Å is low (ca 2 mN/m) indicating that the second adsorbed layer is easily pushed out. Addition of salicylate salt to 0.15 mM C16TASal give rise to a more close packed structure, with a total thickness of 62–65 Å, indicative of a micellar or bilayer arrangement at the surfaces. Furthermore, the frequency dependence of the shear modulus was investigated both at close separation at the innermost force barrier and at larger separations (up to 300–400 Å). The visco-elastic measurements show that the elasticity modulus, G', dominates over the loss modulus, G'', for all studied cases, indicative of a more solid-like than liquid-like film. Finally, it is shown that shear at high contact pressures induces new aggregate structures at the surface.

Keywords: Nanorheology; SFA; Nanostructured films

1. Introduction

1.1. Thin film rheology

During the last 10 years there has been a new development regarding the measurements of surface forces under dynamic conditions: viz. the Surface Force Apparatus, SFA, has been developed to measure dynamic forces [1–3]. Such Surface Force instruments are in general limited to dynamic force measurements between molecular smooth surfaces, preferably two mica surfaces. This restriction has been relaxed however by a French group [4], who studied the dynamic interaction between conducting surfaces.

Only a limited number of studies on visco-elastic properties of thin films using the Tribological Surface Force Apparatus are found in the literature. A rigorous study of thin film rheology (applying a sinusoidal deformation in the lateral direction) of confined polymer melts, using the Tribological Surface Force Apparatus was presented by Luengo et al. [5], where it is shown that confined molecules display different frictional properties than in bulk solution, consistent with previous measurements on thin liquid films [1,2].

When there is an affinity of the surfactants for a surface, which is almost always the case, the surfactants will adsorb and associated surfactant structures at the surface will be spontaneously formed. Recent work using the AFM has shown that surfaces induce different surfactant aggregate packing symmetry [6–11].

The rheology of a lamellar structure, or a dispersion of a lamellar phase in water, is very sensitive to orientational effects. The parallel orientation of the lamellae is not stable in higher shear flow and materials with lamellar structure show a rich variety of shear induced states [12–17]. In the literature it is for example seen that shearing a lamellar system, can cause a transition to a multilamellar vesicle system, MLV, (onion phase) [18,19]. At low shear rates the lamellar phase is oriented with the layers in the shear plane [14]. Whereas at higher shear, the bilayers rotate to an orientation perpendicular to the surface [14].

* Corresponding author. Tel.: +46-8-790-9809; fax: +46-8-20-89-98.
E-mail address: katrin.boschkova@surfchem.kth.se (K. Boschkova).

0301-679X/01/$ - see front matter
PII: S0301-679X(01)00081-0

In this paper results from static and dynamic forces in thin films of aqueous solution of hexadecyltrimethylammonium salicylate (C16TASal) are presented. The cationic surfactant, hexadecyltrimethylammonium salicylate, CTASal, forms cylindrical micelles in bulk aqueous solution at 0.15 and 720 mM there is a transition from cylindrical micelles to a lamellar liquid crystalline phase [20]. In this work the surfactant concentration studied is 0.15 mM, i.e. at the critical micelle concentration, CMC. The surfactants assemble preferentially at the mica surface, driven by the opposite charge of the surfactant headgroup and the mica surface as well as by the hydrophobic effect giving a cooperative adsorption. It is therefore reasonable to assume a liquid crystalline character of the surfactant assembly at the surface [21–23]. In this work it is shown that surfaces that are sheared facilitate the formation of new structured aggregates. In particular it has been shown that cationic surfactants with a salicylate counterion form new aggregates at surfaces after shearing. This observation is in agreement with observations made by, for example, Penfold [14] on associated structures in bulk solution.

The structure of the surfactant assembly at the surface under shear is not clear, since no information about the microstructure is available during the shearing operation. However, from the force curves obtained under non-shear equilibrium conditions, conclusions will be made on the packing of the surfactants at the surfaces and this information is related to the dynamic behaviour. For example, a more close packed layer should have a higher resistance against compression and this should give a higher elasticity modulus, G'.

2. Experimental

2.1. Materials

The C16TASal was obtained by the same methods described in previous papers [24,25]. NaSal was commercially provided. The glue for attaching the mica sheets (see below) was an epoxy resin (Epon 1004), supplied by Shell Chemicals. The water used in the experiments was treated by a Milli-RO 10 Plus pre-treatment unit, including depth filtration, carbon adsorption and decalcination preceding reverse osmosis. This treatment was followed by a Milli-Q plus185 unit, which treats the water with u.v. light (185+254 nm) before a Q-PAK unit consisting of an activated carbon unit followed by mixed bed ion exchanger and finally an Organex cartridge. The outgoing water is filtered through a 0.2 μm filter.

3. Methods

3.1. Measurements of static and dynamic forces of thin films

Surface Force measurements were performed using a surface force apparatus, SFA Mark III [26], (Fig. 1). Two molecular smooth mica sheets (silvered on the backside) were glued with an epoxy resin onto cylindrical silica discs and mounted in a cross-cylindrical configuration in the apparatus.

Visco-elastic measurements were performed by using the bimorph slider attachment (Fig. 1). The bimorphs used were PZT5A, 50 mm long, silver coated from Morgan Matroc Inc. Applying an ac voltage to two parallel piezoelectric bimorph strips induces motion of the lower surface parallel to the contact area. In these experiments a sinusoidal signal was used, with maximum deflection (amplitude) of the lower surface corresponding to 2 μm. The amplitude was chosen to be low in order to assure that the experiments were performed in the linear viscoelastic regime. The response of the upper surface was detected by the friction device. The upper surface was connected to four springs, onto each spring strain gauges are attached. The strain gauges make up the four arms of a Wheatstone bridge. The signal from the friction device was amplified with a strain gauge amplifier (Measurements Group, model 2311). A lock-in amplifier (Stanford Research systems, model SR830) was used to detect the phase between the applied and the detected signal. A lock-in amplifier has the capability to detect and measure very small signals down to a few nanovolts; in this case the external reference used is the signal from the function generator (the signal which is sent to the bimorph). The applied signal from the function generator, the detected response from the friction device and the phase calculated by the lock-in amplifier, were monitored using a Labview program. During the measurements the surfaces were imaged using FECO optical interference technique, which gives continuous information about the local surface geometry and the surface separation.

3.2. Equations of motion for the T-SFA

Upon oscillation the system is described as two coupled damped harmonic oscillators, which Israelachvili has represented by the following equations [5]:

$$\begin{aligned} m_x\ddot{x}+K_x x+\kappa_x\dot{x}+\kappa(\dot{x}-\dot{y})&=F_0e^{i\omega t}\\ m_y\ddot{y}+K_y y+\kappa_y\dot{y}-\kappa(\dot{x}-\dot{y})&=0 \end{aligned} \quad (1)$$

Index x represents the bimorph slider and index y represents the friction device, $(x - y)$ is the relative lateral displacement of the lower and upper surface, m with index refer to the mass, K_x, K_y are the spring constants,

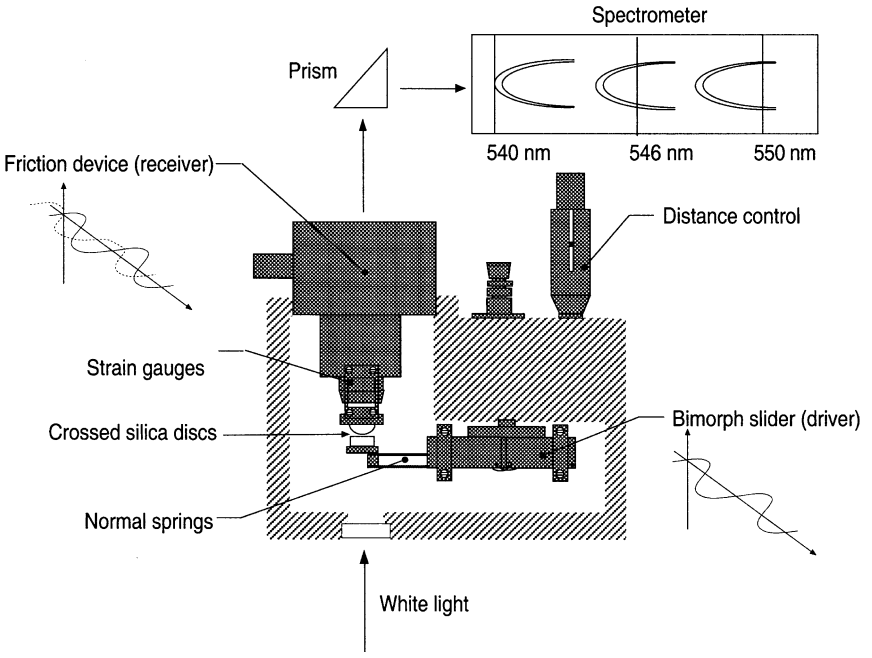

Fig. 1. Schematic illustration of the Tribological Surface Force Apparatus.

κ represents the damping of the film, F_0 is the driving force and ω is the angular frequency. A simplification of the expressions is made assuming that inertia terms can be neglected at frequencies lower than the resonance frequency (which in this case is approximately 200 Hz). It is further assumed that the damping of the driver and the detector can be neglected and the stiffness of the bimorph driver is much larger than for the friction force measuring spring.

Assuming linear viscoelasticity, the viscosity is represented by the complex function, $\eta_{\text{eff}}=\eta'-i\eta''$, where η' is the component that is in phase with the applied strain and η'' is the component which is 90° out of phase. The relation to the storage and loss modulus, G' and G'', is

$$G'=\omega\eta'' \qquad G''=\omega\eta' \tag{2}$$

$$G'=\frac{K_y(f\cos\phi-1)}{\Omega[f^2-(2f\cos\phi-1)]} \qquad G''=\frac{K_y f\sin\phi}{\Omega[f^2-(2f\cos\phi-1)]} \qquad f=\frac{A_0}{A_y} \tag{3}$$

Where f is the relation between the incoming amplitude, A_0, and the detected amplitude, A_y, ϕ is the phase, K_y, is the spring constant of the friction device and Ω is a geometrical parameter. Different geometries define the relation between the frictional force and the damping parameter. The expression for the geometry factor, Ω, is for Reynolds lubrication geometry:

$$F=\kappa v\equiv\Omega\eta v=6\pi R\eta v\left[\frac{8}{15}\log\left(\frac{2R}{D}\right)+\ldots\right]\approx\frac{16}{5}\pi R\eta v\log\left(\frac{2R}{D}\right) \tag{4}$$

where $R\gg D$ (D is the separation and v is the relative velocity) and R is defined as the hydrodynamic radius, related to the cylinder radius R_1 and R_2 by

$$R^2=2(R_1R_2)^{3/2}/(R_1+R_2). \tag{5}$$

In this study a sphere against a flat surface (Reynolds lubrication geometry) is considered, since the contact is not largely deformed in the viscoelastic measurements in the present study.

The assumptions for these equations are (i) a linear response, i.e. a sinusoidal input produces a sinusoidal response and (ii) the viscosities and shear moduli depend only on the frequency and not on the amplitude of the stress or strain.

4. Calibration

4.1. Friction device

The friction device was clamped to a rigid support with the supporting arm in a vertical position. Small weights were placed on the supporting arm and the deflection was measured using a microscope and at the

same time the response from the amplifier-bridge was stored. For each new weight the signal from the Wheatstone bridge was balanced to zero. A mean value for the response of each weight was calculated and then the data was plotted to fit a linear equation defining the force displacement factor. At the same time the stiffness of the spring was calculated from the measured deflection of the spring. Influence of air drafts and temperature drifts were minimised. The procedure was repeated to check for symmetry by rotating the arm 180°.

4.2. Bimorph slider

A voltage was applied to the bimorph slider and the deflection was measured using a microscope. A voltage–displacement factor was defined from a linear fit to the data. The stiffness of the cantilever (lower surface) spring was received from applying weights onto the lower surface and then measuring the deflection using a microscope.

The calibration depends on factors such as glueing, room humidity, the position of the friction device relative to the bimorph in the actual experiment. It is impossible to align the friction device perfectly with respect to the bimorph. In this study, however, comparisons between different systems with a constant set-up of the alignment is made and hence a perfect alignment is not necessary.

5. Results and discussion

5.1. Static forces in thin films

Normal forces between two mica sheets in aqueous solution of C16TASal, with and without NaSal are illustrated in Fig. 2. Measurements in the single surfactant system were performed with a surfactant solution concentration of 0.15 mM, which is the critical micelle concentration (cmc) of the surfactant. The C16TASal system displays an innermost force barrier at a distance of approximately 15–22 Å between the mica sheets. In the light of the fact that the length of the hydrocarbon chain is approximately 20 Å we see the following possible interpretations (see Fig. 3), (i) interdigitated monolayers (ii) patches of monolayers at each surface (iii) a tilted homogenous layer at each surface. The position of the salicylate counterion has been determined by Cassidy et al. [27] and it is suggested that the salicylate ions are intercalated between the molecules and bound to the exterior surface of the micelles.

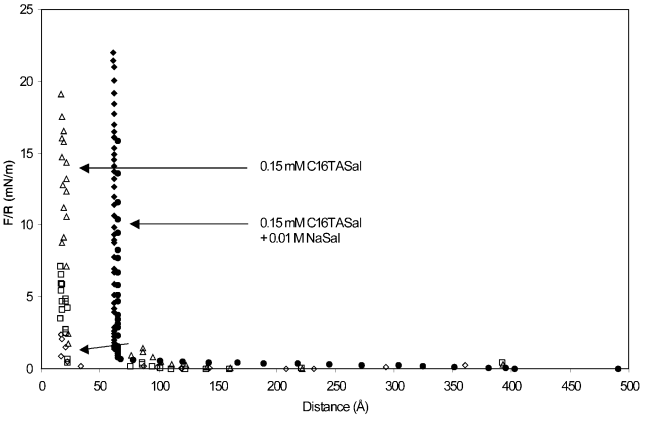

Fig. 2. Force normalised by radius as a function of surface separation between mica surfaces interacting across 0.15 mM C16TASal and 0.15 mM C16TASal+0.01 M NaSal. Two consecutive force runs on approach are plotted.

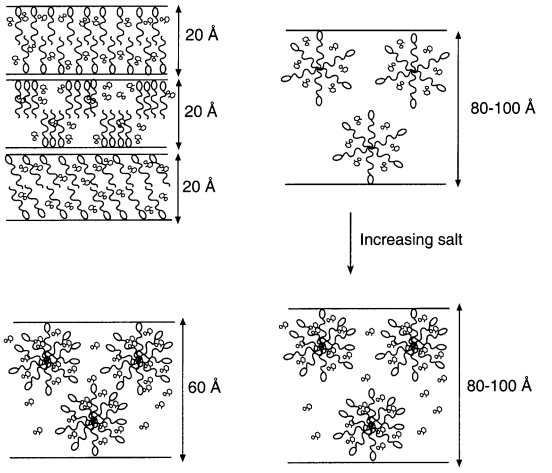

Fig. 3. Schematic picture of possible models for assemblies at the mica surfaces for 0.15 mM C16TASal and 0.15 mM C16TASal+0.01 M NaSal. (The Na^+ ions are not shown in the figure.)

Although the hard wall contact occurs at 22 Å the surfaces experience a weak interaction starting at approximately 100 Å. The interaction increases continuously as the separation decreases to 60 Å, where it is possible to squeeze out the film to the innermost force barrier.

The distance of 100 Å, where the interaction between the surfaces commences, corresponds to a multiple of the theoretical surfactant length, which is 25 Å. This finding can be interpreted in terms of a surfactant bilayer at each surface or a loose packing of micelles at each surface. The observed monotonically increase in the force, as the separation decreases, is due to a compression of the lamellar or micellar structures. The force barrier at a distance at 60 Å is low (ca 2 mN/m) indicating that the second layers are easily pushed out. The height of the force barrier is also an indication of the adsorbed amount. The relative difference between the position of the two force barriers, 40 Å (60–20 Å) is consistent with previous measurements on CTAB using the MASIF [28], where the absolute zero of separation is not accessible and only the separation relative to the ultimate force wall is measured.

It is interesting to note that similar measurements,

using MASIF in salicylate solutions [29], result in a force barrier of 50 Å, which should be compared to the difference, 40 Å, between the barriers at 60 and 20 Å seen here. This significant difference is most likely due to the fact that the temporal regimes of the two experiments are very different. A force curve measurement in the MASIF takes approximately 30 s, whereas the corresponding measurement in the SFA takes 2–3 h. Thus, in the MASIF measurements there is less time for the aggregates to relax into equilibrium structures. Another point of view is that the rapid movement of the surfaces in the MASIF experiments, may induce a new aggregate structure at the surfaces.

For the case, 0.1 mM C16TASal+0.01 M NaSal, there is a force barrier at approximately 62–65 Å, which is equivalent to a compressed bilayer at each surface or a compressed layer of micelles at each surface as in the case above, without salt, see Fig. 2. Upon addition of salt the headgroups will come closer, due to electrostatic shielding of the charged headgroups, resulting in a more tightly packed surfactant layer thereby increasing the resistance against compression and lateral displacement (high force barrier). This, in turn, results in a decreased curvature of the surfactant aggregates whereupon more oblate or cylindrical structures are created. These aggregates, which are formed in the confined film between the mica sheets, are observed in the microscope since they scatter light and also on the interference fringes in the spectrometer. In addition the forces at $F/R<1$ mN/m are not very reproducible, which is interpreted as an effect of aggregate formation.

5.2. Dynamic forces in thin films

5.2.1. Large distance

Fig. 4 shows results from T-SFA oscillatory measurement on relatively thick films of 0.1 mM C16TASal and 0.1 mM C16TASal+0.01 M NaSal at a constant frequency of 10 Hz, (thickness larger than the innermost force barrier). These experiments were performed at fixed distances from 60 to 450 Å, at each distance two consecutive measurements were performed. A mean value of all measurements is given in Fig. 4. The error bars indicate the spread in the results in the measurement regime, i.e. between 60 and 450 Å. The time between measurements was ca 10 min in order to ensure that the system had time to relax. The normal forces were briefly probed to qualitatively ensure that no structural changes took place during shear.

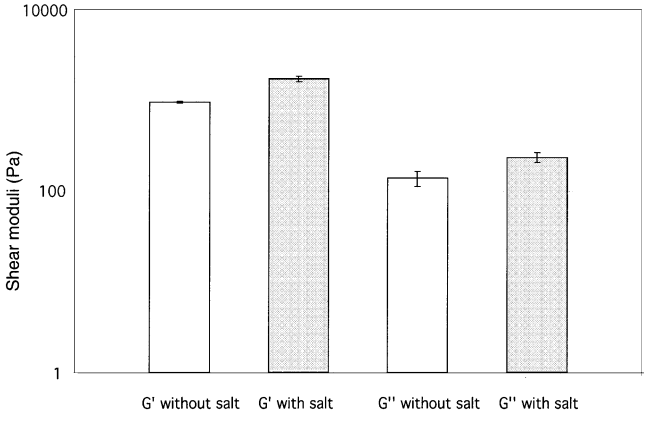

Fig. 4. Shear moduli for 0.15 mM C16TASal and 0.15 mM C16TASal+0.01 M NaSal. Each bar represents an averaged value of measurements at separations between 60 and 450 Å. For each distance, two consecutive measurements were performed. A mean value of all measurements between 60 and 450 Å is displayed.

In both systems (with and without added salt) the shear moduli are constant at separations larger than the hard wall contact position and the elastic contribution (G') dominates over the loss contribution (G''), i.e. the film is more solid-like than liquid-like. Since salt induces a more densely packed surfactant aggregate structure, it is not surprising to note that the storage modulus with added salt is larger than the case without salt. The same data (from Fig. 4) is plotted as an effective viscosity against distance in Fig. 5.

It is also noted that salt also induces new structures in the bulk. In the case of salicylate bulk surfactant systems, long threadlike micelles [30,31] are induced giving rise to solutions, which are visco-elastic due to entanglements. However, implications at surfaces are not known.

5.2.2. Short distance

Measurements of dynamic viscosity were carried out in a frequency range of 1–100 Hz. The frequency dependence on the shear moduli is shown in Fig. 6. These measurements were performed at the innermost force barrier ($F<1$ mN/m), in the case of 0.15 mM CTASal at D=20 Å and for 0.15 mM CTASal+0.01 M NaSal at D=65 Å. Each data-point represents a mean value of two consecutive measurements.

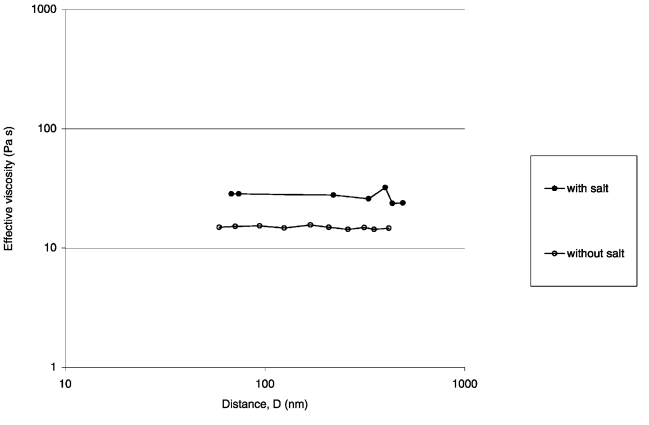

Fig. 5. Effective viscosity vs. distance for 0.15 mM C16TASal and 0.15 mM C16TASal+0.01 M NaSal. The data is recalculated from the original data in Fig. 4.

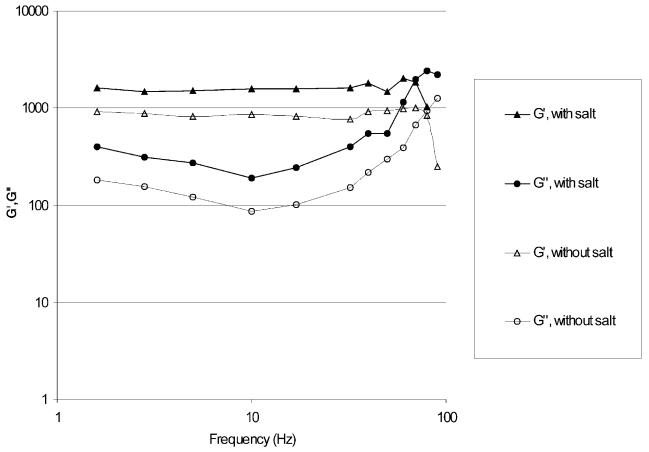

Fig. 6. Shear moduli vs frequency for C16TASal (fixed distance at 20 Å) and 0.15 mM C16TASal+0.01 M NaSal (fixed distance at 60 Å). Each data point represents a mean value of two consecutive measurements.

The slight increase in the shear moduli at higher frequencies is most probably an effect of being close to the resonance frequency of the measurement system, which is estimated to be 200 Hz. This effect is however not seen in the calibration curve for the bimorph slider, probably because the resolution of the calibration is not sufficient. For this first study this is not important since relative differences in shear moduli are being considered. It is observed that in the lower frequency regime, G' and G'' are parallel, indicative of a gel behaviour.

Normally when G' and G'' are plotted versus the frequency there is a crossover point where the two modulii are equal. This crossover point then defines the relaxation time of the system. However, it is not likely that this system can be characterised by only one relaxation time and it is most probable that slower relaxation modes can be found below the measurement frequency window [32]. Fig. 6 indicates that there might be a cross-over point at frequencies much below one Hz, which is the lowest frequency in these measurements.

The same data is plotted as an effective viscosity against shear rate in Fig. 7, where the datapoints above

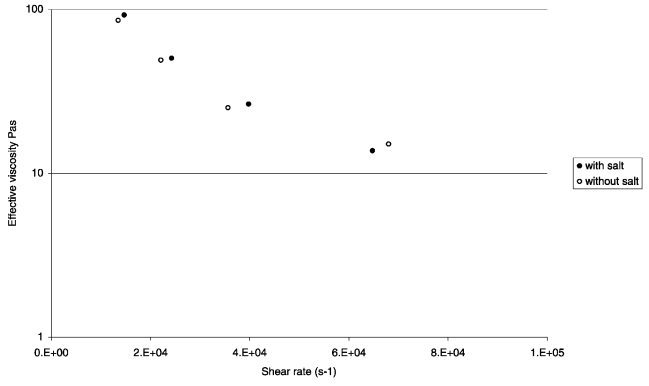

Fig. 7. Effective viscosity vs. shear rate for C16TASal and 0.15 mM C16TASal+0.01 M NaSal. The data is recalculated from Fig. 6.

20 Hz are discarded, since these data are close to the resonance frequency. It is noted that in decreasing the shear rate the effective viscosity increases above the bulk viscosity. This phenomenon is known as a confinement transition. At the displayed shear rates, the relationship between the effective viscosity and shear rate is linear and can hence be described by a power-law behaviour, $\eta_{\text{eff}} \propto \dot{\gamma}^{-a}$. A power law fit for the lower frequencies gives an exponent close to 1 (not shown in Fig. 7), which is in accordance with previous observations by for example Luengo et al. [5]. In the confinement transition region there is a small difference in the effective viscosity parameter due to the addition of salt.

At higher shear rates, viz. above 10^5, the effective viscosity should level off and approach a plateau value. This plateau should in theory [1] correspond to the bulk viscosity. This regime was however not accessible in these experiments.

The system with added salt displays a higher effective viscosity due to a more shear resistant structure, probably also induced by the flow.

5.3. Shear induced structures

Normal force measurements were performed after each set of shearing experiments in order to check the condition of the surfactant layers at the surfaces. These measurements revealed that by performing shear experiments at high contact pressures new structures were induced, which is illustrated in Fig. 8. After shearing, a new force barrier appeared at larger separations, indicating a thicker film. This suggests that the surface film structure has changed. The layer can be removed by a normal force of approximately 20 mN/m and the original force barrier is achieved. Since the pressure at which this happens is still relatively low it is concluded that this is most likely not a structure of a crystalline character. This new structure seems to be nucleated at the surface and

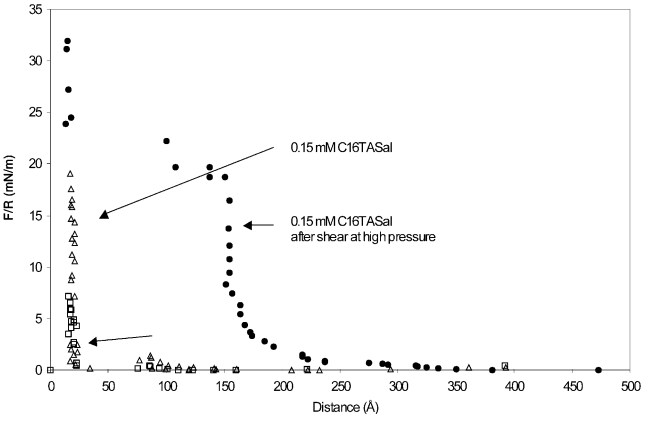

Fig. 8. Force normalised by radius as a function of surface separation between mica surfaces interacting across 0.15 mM C16TASal and 0.15 mM C16TASal+0.01 M NaSal. Forces on approach are displayed before (unfilled symbols) and after shear (filled symbols).

its range increases with time, while the force maximum decreases correspondingly (not illustrated in Fig. 8). It is noted that the thickness of the induced layer corresponds well to the experimental length of rodlike micelles formed in this system (from light scattering data for aqueous 5mM C16TASal using the radius 2.2 nm and aggregation number 61, the length of rodlike micelles can be estimated to be ca 30 nm in aqueous solution [33]).

Upon shearing a lamellar surfactant structure there is an instability resulting in a transition, where the lamellar structure, parallel to the surface, moves to being perpendicular to the surface [14]. Such an instability could explain the different force curves illustrated in Fig. 8. Thus, after shearing at high pressure the bilayers rotate from being first parallel to surface (force barrier at 20 Å), to a perpendicular alignment to the surface (force barrier at ≈200 Å).

6. Conclusions

Static and dynamic behaviour of thin surfactant films in aqueous solution of hexadecyltrimethylammonium salicylate (C16TASal) were investigated using the tribological surface force apparatus. The salt-free surfactant system, 0.15 mM C16TASal, builds up a film of approximately 8–10 Å thickness at each mica surface. Furthermore, the height of the force barrier at 60 Å is low (ca 2 mN/m) indicating that the second adsorbed layer is easily pushed out. Upon addition of salicylate salt to C16TASal a more close packed structure is formed, with a total thickness between the mica sheets of 60 Å. The frequency dependence of the shear modulus was investigated both at close separation, at the innermost force barriers and at larger separations (up to 300–400 Å). Visco-elastic measurements show that the elasticity modulus, G' dominates over the loss modulus, G'', i.e the film behaves more solid-like than liquid-like. Upon addition of salt the structure is more close packed resulting in a higher resistance against compression as well as a higher elasticity modulus.

It is shown that shear at high contact pressures can induce new aggregate structures at the surface. Thus, after shearing at high pressure, the bilayers rotate from being parallel to the surface, to a perpendicular alignment to the surface.

This surface phenomenon is highly interesting for technical applications of shear in boundary regimes, i.e. instead of displaying shear thinning at high contact pressures a thicker film is induced after the shear has stopped, preventing contact and thus wear of the surfaces.

Acknowledgements

We gratefully acknowledge the financial support from the Swedish Research Council for Engineering Sciences and Monbusho-sponsored Japanese Overseas Research Fellowship.

References

[1] Israelachvili JN, McGuiggan PM, Homola AM. Dynamic properties of molecularly thin liquid films. Science 1988;240:189–91.
[2] Van Alsten J, Granick S. Molecular tribometry of ultrathin liquid films. Phys Rev Lett 1988;61:2570–3.
[3] Klein J. Shear, friction, and lubrication forces between polymer-bearing surfaces. Ann Rev Mater Sci 1996;26:581–612.
[4] Georges J-M, Tonck A, Loubet JL, Mazuyer D, Georges E, Sidoroff F. Rheology and friction of compressed polymer layers adsorbed on solid surfaces. J Phys II 1996;6(1):57–76.
[5] Luengo G, Schmitt FJ, Hill R, Israelachvili J. Thin film rheology and tribology of confined polymer melts: contrast with bulk properties. Macromolecules 1997;30:2482–94.
[6] Manne S, Schäffer TE, Huo Q, Hansma PK, Morse DE, Stucky GD, Aksay IA. Gemini surfactants at solid–liquid interfaces: control of interfacial aggregate geometry. Langmuir 1997;13:6382–7.
[7] Patrick HN, Warr GG, Manne S, Aksay IA. Self-assembly structures of nonionic surfactants at graphite/solution interface. Langmuir 1997;13:4349–56.
[8] Jaschke M, Butt HJ, Gaub HE, Manne S. Surfactant aggregates at a metal surface. Langmuir 1997;13:1381–4.
[9] Patrick HN, Warr GG, Manne S, Aksay IA. Surface micellization patterns of quaternary ammonium surfactants on mica. Langmuir 1999;15:1685–92.
[10] Ducker WA, Wanless EJ. Surface-aggregate shape transformation. Langmuir 1996;12:5915–20.
[11] Lamont R, Ducker W. Organized structure of lithium perfluorooctanesulfonate at the graphite–solution interface. J Coll Interface Sci 1997;191:303–11.
[12] Bergenholtz J, Wagner NJ. Formation of AOT/brine multilamellar vesicles. Langmuir 1996;12:3122–6.
[13] Zipfel J, Berghausen J, Lindner P, Richtering W. Influence of shear on lyotropic lamellar phases with different membrane defects. J Phys Chem B 1999;103:2841–9.
[14] Penfold J, Staples E, Lodhi AK, Tucker L, Tiddy GJT. Shear-induced transformations in the lamellar phase of hexaethylene glycol monohexadecyl ether. J Phys Chem B 1997;101:66–72.
[15] Weigel R, Läuger J, Richtering W, Lindner PJ. Anisotropic small angle light and neutron scattering from a lyotropic lamellar phase under shear. J Phys II 1996;6:529–42.
[16] Panizza P, Colin A, Coulon C, Roux D. A dynamic study of onion phases under shear flow: size changes. Eur Phys J B 1998;4:65–74.
[17] Berghausen J, Zipfel J, Lindner P, Richtering W. Shear-induced orientations in a lyotropic defective lamellar phase. Europhys Lett 1998;43:683–9.
[18] Diat O, Roux DJ. Preparation of monodisperse multilayer vesicles of controlled size and high encapsultaion ratio. J Phys II 1993;3(1):9–14.
[19] Escalante JI, Gradzielski M, Hoffmann H, Mortensen K. Langmuir 2000;16:8653–63.
[20] Rao UR. K, Manohar, C., Valaulikar, B.S. and Iyer, R.M., Micellar chain model for the origin of the viscoelasticity in dilute surfactant solutions. J Phys Chem 1987;91:3286–91.
[21] Petrov P, Olsson U, Christenson H, Miklavic S, Wennerström H. Forces between macroscopic surfaces in a sponge phase. Langmuir 1994;10(4):988–90.

[22] Ruths M, Sjöblom J, Blokhus AM. Surfactants and cosurfactants in lamellar liquid crystals and adsorbed on solid surfaces. J Coll Interf Sci 1991;145:108–12.
[23] Blokhus AM, Ruths M, Sjöblom J, Moksheim Andersen O, Ma Z, Friberg SE. Surfactant and cosurfactants in lamellar liquid crystals and adsorbed on solid surfaces IV. Progr Coll Polym Sci 1992;88:63–85.
[24] Imae T, Hashimoto K, Ikeda S. The spinnability of viscoelastic solutions of tetradecyl-trimethylammonium and hexadecyl-trimethylammonium salicylates. Coll Polym Sci 1990;268(5):460–8.
[25] Hashimoto K, Imae T, Nakazawa K. The viscoelasticity of spinnable solutions of alkyltrimethylammonium salicylate. Coll Polym Sci 1992;270:249–58.
[26] Israelachvili JN, McGuiggan PM. Adhesion and short range forces between surfaces. Part I: new apparatus for surface force measurements. J Mater Res 1990;5:2223–31.
[27] Cassidy MA, Warr GG. Surface potential and ion binding in tetradecyltrimethylammonium bromide/sodium salicylate micellar solutions. J Phys Chem 1996;100:3237–40.
[28] Rutland MW, Parker JL. Surface forces between silica surfaces in cationic surfactant solutions: adsorption and bilayer formation at normal and high pH. Langmuir 1994;10:1110–21.
[29] Imae T, Motohisa K, Rutland M. Forces between two glass surfaces with adsorbed hexadecyltrimethylammonium salicylate. Langmuir 2000;16(4):1937–42.
[30] Ulmius J, Wennerström H, Johansson LBÅ, Lindblom G, Gravsholt S. Viscoelasticity in surfactants solutions. J Phys Chem 1979;83(17):2232–43.
[31] Olsson U, Söderman O, Guéring P. Characterization of micellar aggregates in viscoelastic surfactant solutions. J Phys Chem 1986;90:5223–32.
[32] Sollich P. Rheological constitutive equation for a model of soft glassy materials. Phys Rev E 1998;58(1):738–59.
[33] Imae T. Light scattering of spinnable, viscoelastic solutions of hexadecyltrimethylammonium salicylate. J Phys Chem 1990;94:5953–9.